ADVANCED MATERIALS

DOI: 10.1002/adma.200703033

Organic Light-Emitting Nanofibers by Solvent-Resistant Nanofluidics**

By *Carmela De Marco, Elisa Mele, Andrea Camposeo, Ripalta Stabile, Roberto Cingolani,* and *Dario Pisignano**

In the past decade, a lot of attention has been focused on microfluidics for processing and manipulating fluids in channels with dimensions from a few to hundreds of micrometers.[1] Recently, researchers began to investigate the potential of fluidics at the 10–100 nm scale[2] because of its unequalled manipulation, separation, and delivery accuracy at molecular scale, and due to the availability of flexible lithographic techniques[3] for fabricating structures with sub-micrometer resolution. The possibility of controlling the motion of liquids in nanochannels paved the way to the realization of new devices for biological analysis[2b,e] and photonics,[4] improving the spatial resolution and sensitivity in single-biomolecule fluorescent detection, and enabling spectral tunability in nanopatterned optoelectronics. When in nanofluidic channels, molecules with dimensions smaller than their free solution size can be forced to assume a 1D conformation, which allowed the separation of DNA molecules, aiming to replace standard electrophoretic techniques.[2e,f]

In particular, organic, optically, or electrically active 1D nanostructures[5] are attracting increasing attention in view of their integration into sensors and lab-on-a-chip devices, to date necessarily connected to external light sources for fluorescence excitation. These devices would need miniaturized (nanoscale) polarized organic light sources, allowing one to easily decouple excitation and sample emission, thus improving both sensitivity and portability. So far, polarized photoluminescence (PL) has been reported for inorganic nanowires and nanorods,[6] and for molecular materials oriented on substrates,[7] whereas the demonstration of polarized PL for organic 1D nanostructures has been limited to individual self-assembled oligo-(*p*-phenylenevinylene) fibers.[8] The only technique able to fabricate polymeric nanofibers at low cost and with high throughput is electrospinning,[5a,9] which is based on uniaxial elongation of a fluid polymer jet under intense bias. Alternatively, nanofluidic approaches able to meet the simultaneous demands of precise positioning control and chemical flexibility, are very desirable. As active media, conjugated polymers are particularly interesting and have been successfully applied in displays and in solid-state lasers,[10] since they exhibit remarkable PL efficiency and optical gain over the whole visible spectrum and are easily manufactured. However, since conjugated polymers are generally soluble in nonpolar organic solvents such as chloroform and toluene, they require specific, nonswelling-nanofluidic systems. Instead, to date, most nanofluidic experiments have been carried out utilizing silicone-based elastomers such as polydimethylsiloxane (PDMS),[2b,c,4b]] which are known to dramatically swell in nonpolar solvents.[11]

In this work, we demonstrate solvent-resistant nanofluidics as a sub-100 nm technology for building light-emitting organic fibers with precise control of their cross-section and spatial arrangement onto a substrate. Nanofluidics was carried out with optimal resistance to all the organic solvents commonly used for conjugated polymers, to produce optically active nanofibers with a uniform section around 60 nm. The organic fibers were optically characterized in order to assess the preserved functionality of the active polymers after the lithographic step, and were found to exhibit a PL emission polarized along their axis with a polarization ratio of about two.

The material used in the nanofluidic templates was perfluoropolyether (PFPE)-urethane dimethacrylate,[12] which exhibited good resistance to organic solvents. Although standard soft-lithography polymers such as PDMS have been largely applied to micrometer-scale fluidics, and may offer high optical transparency and surface conformability, some of their properties severely limit their potential for nanofluidic applications. PDMS swells significantly in most oil-soluble organic compounds,[11] and its surface energy and Young's modulus are not suitable for sub-100-nm resolution.[12,13] Researchers at IBM proposed that a hard PDMS, obtained from trimethylsiloxy-terminated vinylmethylsiloxane–dimethylsiloxane and methylhydrosiloxane–dimethylsiloxane copolymers,[13b] can be used within composite stamps with a compression modulus of up to 9 MPa. However, this compound is also characterized by poor compatibility with many organic

[*] Dr. D. Pisignano, C. De Marco, Dr. E. Mele, Dr. A. Camposeo, R. Stabile, Prof. R. Cingolani
National Nanotechnology Laboratory of
Istituto Nazionale di Fisica della Materia
Consiglio Nazionale delle Ricerche
c/o Distretto Tecnologico ISUFI via Arnesano
I-73100 Lecce (Italy)
E-mail: dario.pisignano@unile.it
Dr. D. Pisignano, C. De Marco, R. Stabile
Istituto Superiore di Formazione Interdisciplinare
Universitá del Salento via Arnesano
I-73100 Lecce (Italy)

[**] We gratefully acknowledge financial support from the Regional Strategic Project ''Ponamat'' and FIRB Contract RBIP06SH3W. Dr. A. Zompatori and Solvay Solexis are acknowledged for kindly providing the perfluoropolyether-urethane dimethacrylate elastomer. We also thank Dr. A. Cometta and Dr. M. Brich (Zeiss) for the confocal-microscopy measurements.

solvents. De Simone and coworkers recently introduced the use of photocurable PFPE elastomers having surface energies down to 14 mN $m^{-1}$for high-resolution soft lithography.[12] These materials are able to undergo conformal contact onto surfaces, permit easy master release, are compatible with organic-soluble molecules because of the intrinsic oleophobic nature of highly fluorinated materials, and are able to replicate sub-100-nm features with high fidelity. We believe that they can also be widely exploited in the fabrication of chemically flexible, nanometer-scale fluidic systems.

The general validity of the nanofluidic-lithography approach for producing organic nanofibers was tested here for three different conjugated polymers, namely poly[2-methoxy-5-(2-ethylhexyloxy)-1,4-phenylenevinylene] (MEH-PPV), poly[(9,9-dioctylfluorenyl-2,7-diyl)-*co*-(1,4-benzo-{2,1′,3}-thiadiazole)] (F8BT), and poly{(9,9-dioctylfluorenylene-2,7-diyl)-*co*-[1,4-diphenylenevinylene-2-methoxy-5-(2-ethylhexyloxy)-benzene]} (PFV), emitting in the red–orange, yellow, and green regions of the visible spectrum, respectively. A droplet (volume ~1 μL) of conjugated polymer in toluene or chloroform was deposited at the edge of opened nanochannels that were then filled by spontaneous capillarity, leading to the formation of well-aligned light-emitting polymeric features. Channels with cross-section $R = 70$ nm were characterized by a Reynolds number ($\mathrm{Re} = vR\rho/\mu$ where v is the filling velocity, measured to be of the order of 1 mm s^{-1} at the entrance of the nanochannels and of the order of 25 μm s^{-1} during the filling process (Fig. 1), ρ is the density, and μ is the viscosity of the penetrating polymer solution) as low as 10^{-7}, indicating strong laminar flow. The liquid/solid interfacial tension in the channels favors the spontaneous capillary penetration of the organic solution (an image of the contact angle of the MEH-PPV solution on PFPE in presented as the inset of Fig. 1). Solid-state nanofibers were finally achieved after solvent evaporation and peel-off of the mold.

The resultant pattern of aligned polymer fibers with an average cross-section of 66 nm is displayed in Figure 2a, showing very good pattern fidelity (insets of Fig. 2a) and definition, indicating that the resolution achieved can be further increased and depends on the starting master structure. The size distribution of the achieved nanofibers is well fitted by a Gaussian curve of width (full width at half maximum, FWHM) around 20 nm (Fig. 2b). Moreover, the organic fibers maintain a constant section over their length, following the profile of the nanofluidic template. A confocal-microscopy fluorescence image of aligned PFV nanofibers is displayed in the inset of Figure 3. The light output from the nanofibers is clear evidence that the conjugated polymers remain active after the nanofluidic-lithographic process, and that the mold exhibits a good conformal contact with the substrate, permitting the formation of spatially separated sub-100-nm organic fibers. Neither unsought bottom layer nor residual light-emitting polymer between adjacent nanochannels was observed in our experiments. In addition, we were able to obtain isolated light-emitting fibers, or nonwoven meshes of fibers (Fig. 3).

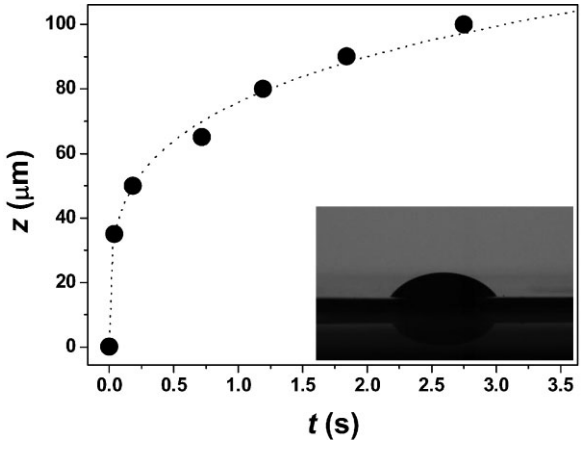

Figure 1. Covered length (z) versus time (t) for the nanofluidic penetration by the conjugated-polymer solution. The dotted line is a guide for the eye. Inset: contact angle image of the employed MEH-PPV solution on a PFPE surface.

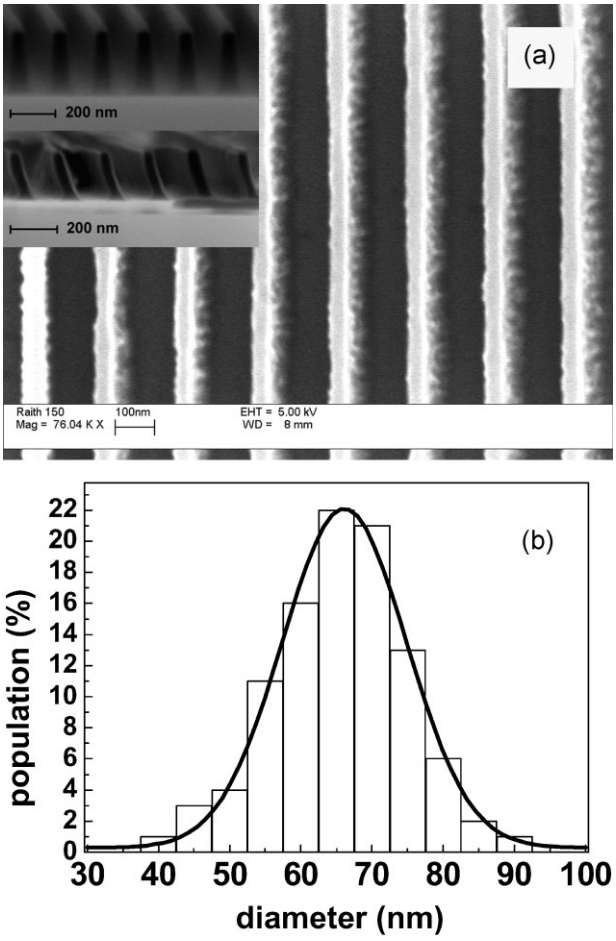

Figure 2. a) SEM image of aligned organic nanofibers. Insets: cross-section view of the employed nanofluidic template (top inset) and resulting aligned-fiber features (bottom inset): feature size and period are about 70 and 200 nm, respectively. b) Size distribution of the produced nanofibers and its fit to a Gaussian.

ADVANCED MATERIALS

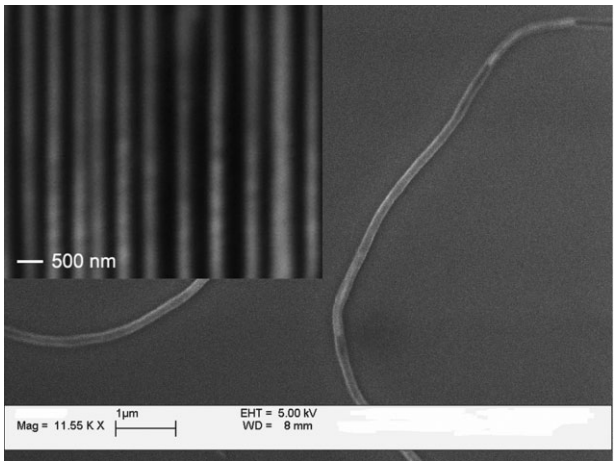

Figure 3. Organic light-emitting nanofibers formed by nanofluidics, with cross-sections of about 160 nm. Inset: Aligned PFV nanofibers imaged by confocal microscopy.

In order to assess the occurrence of changes in spectral properties in the conjugated molecules with respect to bulk solid-state samples, we compared the PL spectra of the nanofibers with those of corresponding spin-cast films (Fig. 4). The PL spectra did not show remarkable variations in their line width, whereas some differences could be observed in the PL peak wavelength, λ_{PL}, which blue-shifts by up to 9 nm for the nanostructures (Table 1). This effect is related to different packing geometries, induced by the laminar molecular flow along the nanofluidic template. Indeed, the photophysical properties of conjugated polymers are remarkably affected by the molecular chain conformation and by their surrounding micro/nanoenvironments, often resulting in PL spectral shifts.[14] The PL-peak wavelength in systems with random

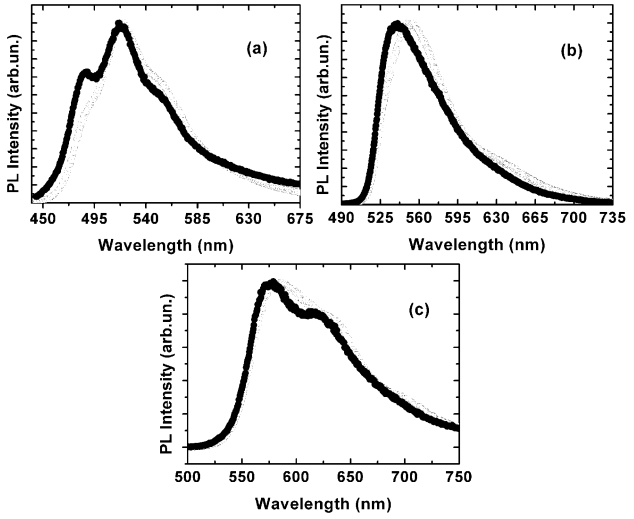

Figure 4. PL spectra of conjugated polymeric films (empty circles) and nanofluidic nanofibers (superimposed solid lines) for a) PFV, b) F8BT, and c) MEH-PPV.

Table 1. Emission peak wavelength, λ_{PL}, and linewidth (FWHM, $\Delta\lambda_{PL}$) of conjugated polymers in spin-cast films and nanofibers.

	Spin-cast film		Nanofibers	
Compound	λ_{PL} [nm]	$\Delta\lambda_{PL}$ [nm]	λ_{PL} [nm]	$\Delta\lambda_{PL}$ [nm]
MEH-PPV	583	103	579	102
F8BT	550	64	541	65
PFV	520	82	516	87

coil conformation of polymer chains decreases with respect to that in denser samples, resulting in more compact packing and extended π–π overlap between different conjugated segments.[14a,d,f] Excitation migration towards lower-energy chromophores determines red-shifted, narrower luminescence spectra instead.[14h,i] Moreover, purely optical size-dependent confinement effects are often observable, such as in the case of thickness-dependent gain-narrowing in polymer films exhibiting amplified spontaneous emission, for which smaller thickness values induce reduced waveguiding of high-wavelength spectral components, and hence blue-shift of the spectra.[15] In our experiments, we found a blue-shift of the PL-peak wavelength from spin-cast films to nanofibers, which can be related to the corresponding decrease in thickness of the light-emitting organic material and to the concomitant energy-migration suppression.

In some species (see for instance the MEH-PPV and PFV spectra reported in Fig. 4), we also observed better-defined spectral vibronic progressions for nanofluidic samples than in spin-cast films. This last effect suggests that the nanofluidic filling leads to an enhancement of the molecular order and alignment in the nanochannels. In fact, since conjugated polymers emit preferentially along transition dipole moments, collinear to radiative conjugated segments, and along molecular chains (deviations within about 20° have been reported),[16] such flow-induced orientation of molecules within mutually aligned organic nanofibers can be exploited to obtain devices with macroscopic optical anisotropy. To investigate this issue, we analyzed the polarization state of the nanofiber emission. Figure 5 shows the normalized PL intensity (I) transmitted through a polarizer as a function of the angle (θ) between the polarizer axis and the grating grooves, and the corresponding fit to Malus' law $I = I_0 \cos^2(\theta + \phi) + I_1$, where I_0 and I_1 indicate the intensity of the polarized component of the emission and of the unpolarized background, respectively and ϕ is a phase angle. For comparison's sake, we also show the behavior of the PL emission from a spin-cast film, which is almost independent of collection angle. Instead, the measured polarization ratio, $R = I_{\parallel}/I_{\perp}$, between the intensities parallel ($I_{\parallel}$) and perpendicular ($I_{\perp}$) to the nanofiber axis is about 2,[17] confirming that a partial alignment occurs along the channel direction due to laminar nanofluidic flow, and as a consequence, the transition moments of the molecular-conjugation segments are also mainly aligned along the fiber axis.

In conclusion, we demonstrate solvent-resistant nanofluidics as a straightforward, low-cost, and chemically flexible method for producing organic light-emitting nanofibers. Nanofluidics,

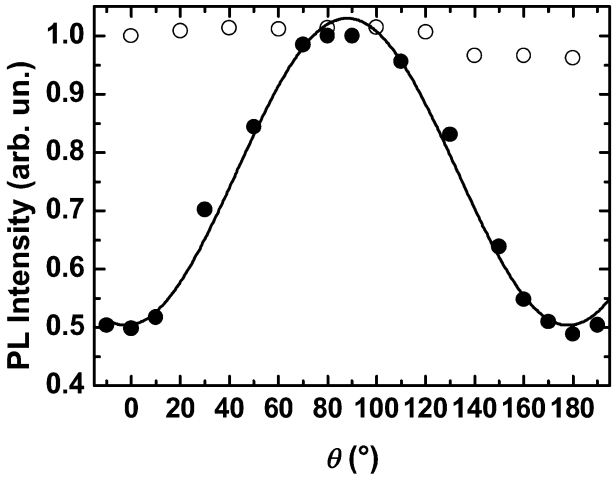

Figure 5. Polarization-dependent PL of uniaxially aligned conjugated-polymer nanofibers: dependence of the output intensity of film (empty circles) and of nanofibers (full circles) on the angle (θ). For the organic nanofibers, θ is the angle between the polarizer axis and the grating grooves. The solid line is a fit of the data to Malus' law.

with its unique fluid-manipulation characteristics, allows one to place nanofibers in a specific region of a solid substrate with precision and with highly controlled cross-sections. This method concomitantly minimizes the broadening of molecular-chain conformations and favors orientation through the nanochannels, in a simple way with major advantages over other methods that require complex alignment procedures. Light-emitting fibers were successfully fabricated with different conjugated polymers, with cross-sections around 60 nm and polarization ratios of about 2 for the PL emission. These results open a new perspective for the realization of polarized light-sources for nanophotonics, sensors, and lab-on-a-chip devices.

Experimental

Materials: The three different light-emitting conjugated polymers used were purchased from American Dye Source Inc. (Quebec, Canada): MEH-PPV, F8BT, and PFV. These light-emitting materials have their PL emission respectively in the orange (583 nm), yellow (550 nm), and green (520 nm) regions of the visible spectrum. For all conjugated polymers, we prepared a toluene solution (0.86% w/v).

PFPE-urethane-methacrylate was kindly provided by Solvay Solexis (Italy), and the 2-hydroxy-2-methylpropriophenone photoinitiator (Darocur® 1173), used in the fabrication of PFPE elements, was obtained from Ciba (Italy). For the cured PFPE surfaces, we estimated a surface energy $\cong$15 mN m^{-1} by water contact-angle measurements. The organic solvents chloroform and toluene, employed in the preparation of solutions of conjugated polymers, were purchased by J. T. Baker (Phillipsburg, NJ).

Fabrication of Master Structures: The master structures, characterized by parallel grooves with period = 200 nm and feature width of about 70 nm, were produced by electron-beam lithography using a Raith150 system. A poly(methyl methacrylate) positive-electronic resist was spin-cast on a Si (100) n-type substrate, obtaining a thickness of about 100 nm. The resist was then exposed to an electron beam with acceleration energy of 5 keV and beam current of 30 pA for a total exposed area of 1 mm^2. The development of the resist was carried out with a methylisobutylketone (MIBK)/isopropyl alcohol (IPA) 1:3 solution for 1 min. Afterwards, 15 nm of Cr were thermally evaporated onto the substrate surface. Finally, after the Cr lift-off carried out in acetone for 30 min, the substrate was exposed to Ar and CF_4 plasma for reactive ion etching.

Nanofluidics: The geometry of the master was faithfully replicated by the PFPE elastomer. The PFPE-prepolymer was obtained by mixing the PFPE-urethane dimethacrylate with 4% w/w of the photoinitiator. PFPE molds were produced by spin-coating the prepolymer on the master (400 rpm for 40 s) and irradiating it with UV light ($\lambda \sim$360 nm, delivered by two 6 W lamps for 30 s at a distance of 10 cm from the sample), under inert nitrogen atmosphere. The PFPE mold, peeled off from the master, was placed in contact with a Si wafer, in order to have opened capillaries with lateral dimension of 70 nm, constituted by three PFPE walls and one Si wall. For nanofluidics, a 1 μL droplet of conjugated-polymer solution was deposited close to the opened channels, which were filled by spontaneous capillarity. For our channel geometry, the wettability from the organic solution is different along the different capillary walls, with liquid-surface contact angles $\alpha_{PFPE} = 47^\circ \pm 1^\circ$ (inset of Fig. 1) and $\alpha_{Si} = 28^\circ \pm 1^\circ$, respectively (as measured using an Optical Video Contact-Angle System CAM-200 KSV). Both contact angle values, α_{PFPE} and α_{Si}, are in agreement with spontaneously occurring capillary filling. The PFPE mold was removed after about 12 h, ensuring complete solvent evaporation.

The filling rate of the liquid front during the capillary rise was observed by optical microscopy through a fast camera (FastCam APX-RS, Photron). The exact position of the fluid front along the nanochannels during the entire filling process was determined by an acquisition rate of 250 frames s^{-1} using dedicated viewer software. The system temperature was kept constant at 293 K during nanofluidics. The nanofluidic filling rates monotonously decrease from an initial value of about 1 mm s^{-1}, at the entrance of nanochannels, down to the order of 10 μm s^{-1} for a penetration coordinate of 100 μm.

Scanning Electron Microscopy (SEM) and Confocal Microscopy Characterization: SEM investigation was performed using a Raith150 electron-beam system operating with an acceleration voltage of 5 kV and an aperture size of 30 μm. Confocal microscopy was carried out using an Axio Observer inverted microscope equipped with a LSM510-23META head (Zeiss), exciting the nanofibers with an Ar laser ($\lambda = 488$ nm).

Optical Characterization: PL emission spectra from both bare films and nanofibers were collected by exciting the samples with a diode laser (Nichia, Japan) emitting at 405 nm with an output power up to 60 mW, and using a fiber-coupled monochromator (iHR320, Jobin Yvon) equipped with a charge-coupled device detector (Simphony, Jobin Ivon). All the measurements were carried out at room temperature.

Received: December 6, 2007
Revised: April 11, 2008

[1] a) T. M. Squires, S. R. Quake, *Rev. Mod. Phys.* **2005**, *77*, 977. b) G. M. Whitesides, *Nature* **2006**, *442*, 368.

[2] a) T. Becker, F. Mugele, *Phys. Rev. Lett.* **2003**, *91*, 166104. b) R. Mukhopadhyay, *Anal. Chem.* **2006**, *78*, 7379. c) D. Huh, K. L. Mills, X. Zhu, M. A. Burns, M. D. Thouless, S. Takayama, *Nat. Mater.* **2007**, *6*, 424. d) J. Fu, R. B. Schoch, A. L. Stevens, S. R. Tannenbaum, J. Han, *Nat. Nanotechnol.* **2007**, *2*, 121. e) S. W. P. Turner, M. Cabodi, H. G. Craighead, *Phys. Rev. Lett.* **2002**, *88*, 128103. f) J. Han, H. G. Craighead, *Science* **2000**, *288*, 1026.

[3] B. D. Gates, Q. Xu, M. Stewart, D. Ryan, C. G. Willson, G. M. Whitesides, *Chem. Rev.* **2005**, *105*, 1171.

ADVANCED MATERIALS

[4] a) D. Psaltis, S. R. Quake, C. Yang, *Nature* **2006**, *442*, 381. b) D. Erickson, T. Rockwood, T. Emery, A. Scherer, D. Psaltis, *Opt. Lett.* **2006**, *31*, 59.
[5] a) A. Babel, D. Li, Y. Xia, S. A. Jenekhe, *Macromolecules* **2005**, *38*, 4705. b) A. N. Aleshin, *Adv. Mater.* **2006**, *18*, 17. c) J. M. Moran-Mirabal, J. D. Slinker, J. A. DeFranco, S. S. Verbridge, R. Ilic, S. Flores-Torres, H. Abruna, G. G. Malliaras, H. G. Craighead, *Nano Lett.* **2007**, *7*, 458.
[6] a) J. Wang, M. S. Gudiksen, X. Duan, Y. Cui, C. M. Lieber, *Science* **2001**, *293*, 1455. b) J. Hu, L. S. Li, W. Yang, L. Manna, L. W. Wang, A. P. Alivisatos, *Science* **2001**, *292*, 2060.
[7] M. Grell, D. D. C. Bradley, *Adv. Mater.* **1999**, *11*, 895.
[8] C. R. L. P. N. Jeukens, P. Jonkheijm, F. J. P. Wijnen, J. C. Gielen, P. C. M. Christianen, A. P. H. J. Schenning, E. W. Meijer, J. C. Maan, *J. Am. Chem. Soc.* **2005**, *127*, 8280.
[9] D. Li, Y. Xia, *Adv. Mater.* **2004**, *16*, 1151.
[10] a) N. Tessler, G. J. Denton, R. H. Friend, *Nature* **1996**, *382*, 695. b) A. Kraft, A. C. Grimsdale, A. B. Holmes, *Angew. Chem. Int. Ed.* **1998**, *37*, 402.
[11] J. N. Lee, C. Park, G. M. Whitesides, *Anal. Chem.* **2003**, *75*, 6544.
[12] J. P. Rolland, E. C. Hagberg, G. M. Denison, K. M. Carter, J. M. De Simone, *Angew. Chem. Int. Ed.* **2004**, *43*, 5796.
[13] a) E. Delamarche, M. Schid, M. A. Richuyck, R. Michael, *Adv. Mater.* **1997**, *9*, 741. b) H. Schmid, B. Michel, *Macromolecules* **2000**, *33*, 3042.
[14] a) T. Q. Nguyen, R. Y. Yee, B. J. Schwartz, *J. Photochem. Photobiol. A: Chem.* **2001**, *144*, 21. b) T. Q. Nguyen, B. J. Schwartz, *J. Chem. Phys.* **2002**, *116*, 8198. c) C. J. Collison, L. J. Rothberg, V. Treemaneekarn, Y. Li, *Macromolecules* **2001**, *34*, 2346. d) T. Q. Nguyen, V. Doan, B. J. Schwartz, *J. Chem. Phys.* **1999**, *110*, 4068. e) I. D. W. Samuel, G. Rumbles, C. J. Collison, S. C. Moratti, A. B. Holmes, *Chem. Phys.* **1998**, *227*, 75. f) M. Zheng, G. L. Bai, D. B. Zhu, *J. Photochem. Photobiol. A: Chem.* **1998**, *116*, 143. g) M. Yan, L. J. Rothberg, E. W. Kwock, T. M. Miller, *Phys. Rev. Lett.* **1995**, *75*, 1992. h) G. Padmanaban, S. Ramakrishnan, *J. Am. Chem. Soc.* **2000**, *122*, 2244. i) D. Hu, J. Yu, G. Padmanaban, S. Ramakrishnan, P. F. Barbara, *Nano Lett.* **2002**, *2*, 1120.
[15] A. K. Sheridan, G. A. Turnbull, A. N. Safonov, I. D. W. Samuel, *Phys. Rev. B* **2000**, *62*, 11929.
[16] G. R. Hayes, I. D. W. Samuel, R. T. Phillips, *Phys. Rev. B* **1997**, *56*, 3838.
[17] A similar value of R is reported in the literature for self-assembled nanofibers. See ref.[8].